



Decoupling Between the Atmosphere and the Underlying Surface During Stable Stratification

Thomas Foken¹

Received: 3 April 2022 / Accepted: 29 August 2022 / Published online: 28 September 2022
© The Author(s) 2022

Abstract

Strong temperature gradients with stable stratification immediately above the surface are typical for radiation cooling, but near-surface temperature inversions (hereinafter referred to as inversions) have hardly been studied. Both phenomena are examined in more detail by means of measurements in the Caspian Sea and Antarctica and compared with measurements made by other authors. For this purpose, tests for decoupling are applied in the first case. In the second case, the inversions can be explained in the context of counter-gradient fluxes and turbulent Prandtl numbers greater than one.

Keywords Decoupling · Richardson number · Stable stratification · Surface layer · Turbulent Prandtl number

1 Introduction

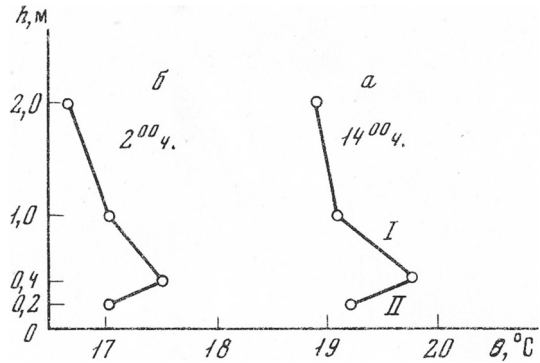
In the case of rare meteorological phenomena, it sometimes takes a very long time until sufficient measurement data are available to describe these events reliably and, where possible, link them to a theory. This paper describes a possible decoupling of the near-surface air layer of a maximum thickness of a few metres from the overlying atmosphere. I first became aware of this in 1975 when I participated in a discussion with Prof. Chundshua at the Institute of Physics of the Atmosphere in Moscow, in which Prof. A. M. Obukhov also took part. The basis for the discussion was the work of Chundshua and Andreev (Andreev et al. 1969; Chundshua and Andreev 1980) in which a near surface temperature inversions (hereinafter referred to as inversions) were found during temperature measurements made by Moscow University in 1969 over the Black Sea near the water surface (Fig. 1). However, initial findings are also shown in Bruch's measurements in the Baltic Sea (Bruch 1940). The discussion did not lead to a conclusive explanation, even though Chundshua and Andreev (1980) assumed chemical binding energy to be the cause.

In 1975 and 1976, I conducted temperature profile measurements in the Caspian Sea to study the molecular boundary layer above the sea (Foken et al. 1978; Foken 2002). A

✉ Thomas Foken
thomas.foken@uni-bayreuth.de

¹ Bayreuth Center of Ecology and Environmental Research, University of Bayreuth, 95440 Bayreuth, Germany

Fig. 1 Vertical temperature profile over the Black Sea during the day 1400 (a) and night 0200 (б), from Chundshua and Andreev (1980)



dropsonde was used (Foken 1975), whereby only the lowest 20 cm above the sea were measured with very high spatial resolution. In 1976, some measurements were also made within the lowest 10 m, with results similar to those from the measurements in the Black Sea (Sect. 3). It was not possible to publish these results in the journal *Fizika Atmosfery i Okeana* because “the measurements contradict the Monin–Obukhov similarity theory and thus must be wrong”. They were published in a German institute journal (Foken and Kuznecov 1978).

Inversions of about the same height and magnitude have also been observed over melting snow in the French Alps and near Madrid (de La Casinière 1974), and over snow in the Californian Sierra Nevada mountain range (Halberstam and Schieldge 1981). In both experiments, only temperature profile measurements exist. Evaporation or sublimation at the surface is assumed to be the cause. With reference to this work, King and Anderson (1994) also suspected similar cases in their measurements at the Halley Research Station, Antarctica, in 1991, but lack of measurements at low heights did not permit a precise conclusive statement. This was also true for measurements made in 1986 at the same location (King 1990). However, for the first time, these authors suggest that, under such conditions, the coefficients in the profile functions for momentum are larger than those for heat whereas this is usually the other way round. An increase in the turbulent Prandtl number was also later demonstrated for the experiment in 1986 for very stable stratification and low friction velocities at heights of ≥ 5 m (Yagüe and Cano 1994; Yagüe et al. 2001). An overview of the magnitude of the turbulent Prandtl number was given by Andreas (2002) that incorporated the results of King et al. (1996); he found that, predominantly, the turbulent Prandtl number is limited at $\text{Pr}_T = 1$. Obviously hardly noticed, was an evaluation of the SHEBA experiment conducted from October 1997 to October 1998 (Persson et al. 2002) in the Arctic by Grachev et al. (2007), which showed turbulent Prandtl numbers significantly greater than one with increasing stability. Remarkable in this work is a discussion of self-correlation.

In the FINTUREX (FINAL TURbulence EXperiment of the Meteorological Main Observatory, Potsdam) campaign conducted at the Neumayer II Station in Antarctica, I examined the problem again, although the experiment itself served to determine the height of the stable boundary layer and universal functions (Handorf et al. 1999; Sodemann and Foken 2004). It was found that some data were unusable for the studies when the stratification was very stable. This led to the extension of a data quality test for eddy-covariance measurements, with respect to the stationarity of the measurement conditions (Gurjanov et al. 1984) by testing the development of the turbulence (Foken and Wichura 1996) by means of integral turbulence characteristics (normalized standard deviations), as it is widely used today in most programs of flux calculation according to the eddy-covariance method. The measurements

at very stable stratification were specially evaluated with a time delay (Sodemann and Foken 2005) and are presented in Sect. 3. It must be noted that, on the recommendation of John King (British Antarctic Survey), the measurement heights below 5 m were added in comparison to the Halley experiment.

The first summary of the measurements in the Caspian Sea and the Antarctic appeared in a German publication (Foken 2003). However, a theoretical explanation of the effects found was missing. In the meantime, decoupling has been assumed as a possible cause. This phenomenon is known for plant stands, when Kelvin–Helmholtz instabilities form due to the high roughness and generated coherent structures are the cause of the coupling of the trunk space with the atmosphere (Raupach et al. 1996; Finnigan 2000; Thomas and Foken 2007). In some cases, counter gradients even occur in the canopy (Denmead and Bradley 1985). An overview was recently given by Brunet (2020). From this, various approaches developed to account for the coupling when studying the interaction between forests and the atmosphere (Thomas and Foken 2007; Jocher et al. 2017; Peltola et al. 2021). A similar decoupling was also found at the forest floor (Sörgel et al. 2017). Jocher et al. (2017) developed a method using the standard deviation of the vertical wind component for high vegetation. A use of this standard deviation to determine the coupling was recently proposed by Peltola et al. (2021) for low vegetation as well.

The previous theoretical observations always originated from Monin–Obukhov similarity theory. This is based on a largely constant turbulent Prandtl number and allowed modifications for more stable stratification only by modifying the universal functions (Foken 2006). For the present case, a new approach is of interest, which assumes $Pr_T \gg 1$ for strongly stable stratification (Zilitinkevich et al. 2013; Basu and Holtlag 2021). These assumptions and the decoupling are discussed below in the interpretation of the phenomena found.

2 Material and Methods

2.1 Experimental Data

The KASPEX-76 experiment took place from 1 to 27 April 1976, on a former oil drilling platform in the Caspian Sea (Fig. 2a) at a distance of 25 km offshore and at a water depth of 40 m (coordinates approx. 40°30' N and 50°45' E). Several measurements with a dropsonde (Foken 1975) provided snapshots of the vertical fine structure of the air temperature profile for selected situations. The dropsonde was equipped with a platinum resistance sensor with a diameter of 2 μm and a dropping speed of 1 m s^{-1} . The standard meteorological instruments were in-house constructions of the Institute of Oceanology, Moscow. The sonic anemometer worked according to the phase difference method (Bovsheverov and Voronov 1960; Koprov 2018).

FINTUREX took place from 18 January to 19 February 1994 at the Neumayer II Station, Antarctica (70°39' S, 8°15' W) (Fig. 2b) during the polar day. The station is situated on the Ekström Ice Shelf at 42 m above sea level and the terrain is completely flat within a radius of several kilometres and was not disturbed by significant zastrugi even at close range (200–400 m). Thus, vertical divergences of the sensible heat flux due to the surface conditions should be excluded. Profiles of wind speed and temperature were measured using a profile tower with various measurement heights between 0.5 and 10 m (Table 1). For further details like quality control and data calculation, see Handorf et al. (1999) and Sodemann and Foken (2005). For quality control, the method by Foken and Wichura (1996) was used for

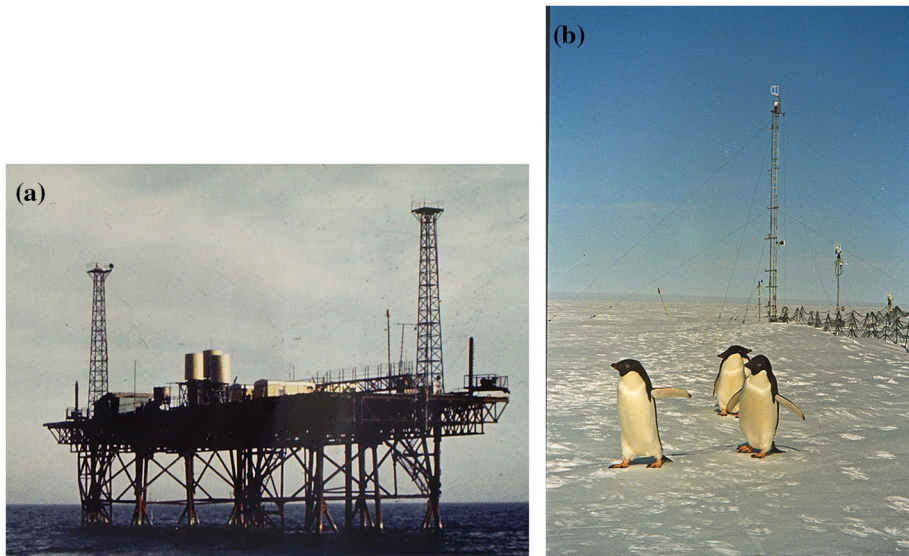


Fig. 2 Measurement platform of the Azerbaijan Academy of Sciences during KASPEX-75,76 (a), and installation of the three turbulence measurement complexes and profile measurements during FINTUREX (b) (photos: Foken)

Table 1 Instrumentation during FINTUREX (Handorf et al. 1999, completed and relevant measurements only)

Meteorological parameter	Height of the sensor, m	Instrument
Fluctuations of sonic temperature, horizontal and vertical wind velocity	1.7, 4.2, 11.6	Kaijo–Denki sonic anemometer, Probe A, DAT 310, Hanafusa et al. (1982)
Wind speed	0.5, 1.0, 2.0, 3.1, 4.5, 6.0, 8.0, 10.0	Cup anemometer, Brömme et al. (1991)
Temperature (only dry temperature was used)	0.5, 1.0, 2.0, 4.5, 10.0	Psychrometer, ventilated and radiation-shielded, Baum et al. (1994)
Shortwave radiation, up- and downwelling	2.0	CM14 Kipp & Zonen
Longwave radiation, up- and downwelling	2.0	Schulze–Däke, Däke (1972)

the first time, thus excluding non-steady-state measurements and those that did not meet similarity criteria for developed turbulence. The reported sensible heat fluxes are, strictly speaking, buoyancy fluxes, since sonic temperature was used. No correction was applied because of the small differences to the thermodynamic temperature in the relevant humidity range. Likewise, the temperatures of the profile measurements were not converted to potential temperatures because of the too small differences in the height range of interest < 5 m.

Because of data storage limitations, original data are no longer available for experiments conducted ≥ 30 years ago. Since the following evaluations refer to already processed mean

data for usually 30-min intervals, some evaluation procedures must be omitted, so that the presentation of the corresponding theories does not take place here, like the investigation of the coupling by means of wavelet analyses (Thomas and Foken 2007).

2.2 Theoretical Background

2.2.1 Decoupling Detection with Critical Vertical Wind Velocity

Unfortunately, for KASPEX-76, only a phenomenological interpretation is possible. However, a simplified coupling scheme for FINTUREX could be applied with the standard deviation of the vertical wind component (σ_w) proposed by Peltola et al. (2021) for lower vegetation as well. They defined a critical vertical speed (w_{crit}) that experimental studies (Mahrt et al. 2013; Acevedo et al. 2016) showed to be dependent on the height and the Brunt–Väisälä frequency. For coupled conditions:

$$\sigma_w > w_{\text{crit}} = 0.61\sqrt{2z}N, \quad (1)$$

are assumed, where:

$$N = \sqrt{\frac{g}{\theta} \frac{\partial \theta}{\partial z}}, \quad (2)$$

is the Brunt–Väisälä frequency (θ : potential temperature, g : the acceleration due to gravity, z : height).

2.2.2 Decoupling Detection with Model Calculations

The demonstration of decoupling was performed for FINTUREX by Sodemann and Foken (2005), using a hydrodynamic multilayer model. It was also applied in the same way by Lüers and Bareiss (2010) over snow, and by Sörgel et al. (2017) near the forest floor. The model is based on the model by Foken (1979; 1984; 2002), where the exchange coefficient is determined separately for the molecular boundary layer, the buffer layer and the turbulent neutral and stratified surface layer:

$$\overline{w'\theta'} = \left(\int_0^z \frac{dz}{K_h + \nu_{Tt} + \nu_T} \right)^{-1} [\theta(z) - \theta_0], \quad (3)$$

where ν_{Tt} is the molecular-turbulent diffusion coefficient of the buffer layer and ν_T is the molecular temperature diffusion coefficient of the molecular sublayer. The diffusion coefficients based on parametrizations obtained from the investigations of the molecular boundary layer during the KASPEX experiments (Foken 1978; Foken et al. 1978). Similar models were developed by Sverdrup (1936, 1937/38, two-layer model) and Bjutner (1974, three-layer model). Recently, a similar two-layer model was published by Gross (2021). Note: In the Sodemann and Foken (2005) paper, there is an error in the model equations. The correct model equations appear in the original paper (Foken 1979) or in Lüers and Bareiss (2010). The software tool used was not affected by the error.

2.2.3 Theory of Strong Stable Stratification

In contrast to Monin–Obukhov’s similarity theory, the theoretical approach of Zilitinkevich et al. (2013) describes a dependence of the exchange on a non-constant turbulent Prandtl

number for stable stratification:

$$Pr_T = \frac{K_m}{K_h} \gg 1, \tag{4}$$

(K_m and K_h are the exchange coefficients for momentum and heat) for gradient Richardson numbers as a bulk definition:

$$Ri = \frac{g}{\theta} \frac{[\theta(z) - \theta_0]z}{[u(z)]^2} > 1, \tag{5}$$

with the potential temperature at the surface θ_0 and the wind speed u . For strongly stable stratification, this implies a significantly suppressed heat exchange compared to momentum transfer. Thus, the model describes a non-gradient-based closure approach for turbulent fluxes. For the following investigations, the equation:

$$Ri = Ri_f Pr_T, \tag{6}$$

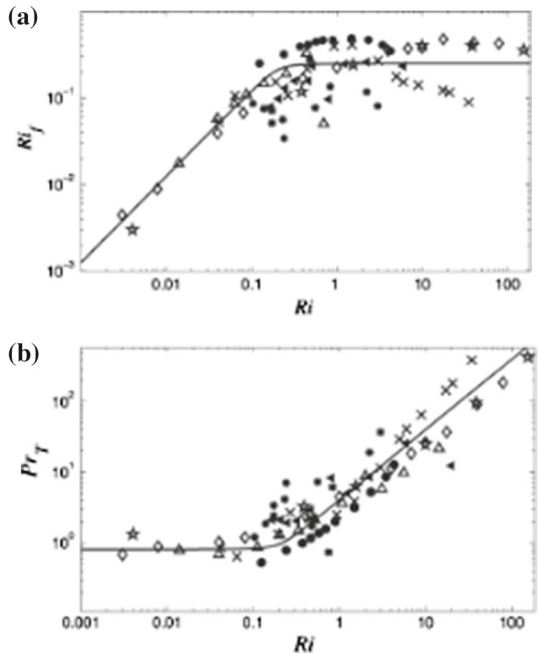
with the flux Richardson number:

$$Ri_f = \frac{g}{\theta} \frac{\overline{w'\theta'}}{\overline{w'u'}(\partial u/\partial z)}, \tag{7}$$

($\overline{w'\theta'}$ is the kinematic sensible heat flux and $\overline{u'w'}$ is the momentum flux with w the vertical velocity component) shown in Fig. 3 is relevant. The eddy viscosity and the eddy conductivity are calculated according to:

$$K_m = -\frac{\overline{w'u'}}{\partial u/\partial z}, \tag{8}$$

Fig. 3 Dependence of gradient Richardson number Ri on flux Richardson number Ri_f (a) and turbulent Prandtl number Pr_T (b) according to Zilitinkevich et al. (2013), where symbols represent measured data, large-eddy simulation (LES) and direct numerical simulation (DNS) model results. The line is the Energy- and Flux-Budget Turbulence Closure Model developed by the authors and is described by Eq. (6)



and:

$$K_h = -\frac{\overline{w'\theta'}}{\partial\theta/\partial z}. \tag{9}$$

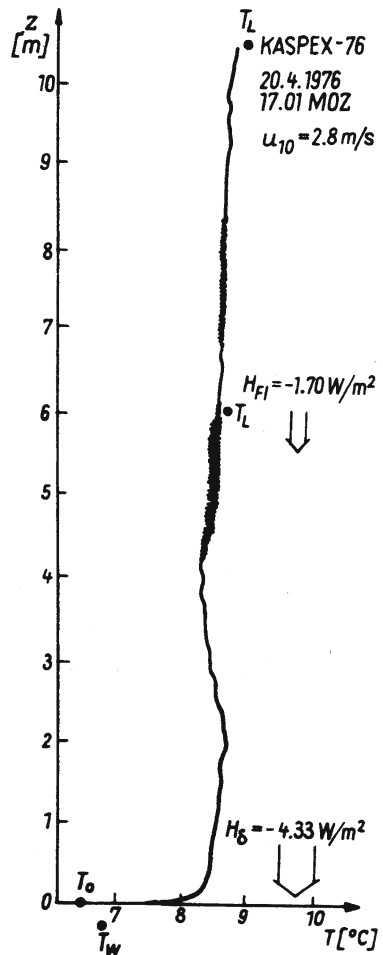
Because of Eq. (6), it is obvious that the graphs shown in Fig. 3 are influenced by self-correlation, as studied by Grachev et al. (2007, 2012). However, the ratio of the exchange coefficients defined in Eqs. (8) and (9) and thus the size of the turbulent Prandtl number is relevant for the present investigation.

3 Experimental Findings

3.1 Results of the KASPEX-76 Campaign

Only a few soundings with the dropsonde are available from KASPEX-76 (Fig. 4). The stable cases show the inversion layer at a height of about 2 m. A region of increased turbulence

Fig. 4 Vertical temperature profile on at 1701 LT on 20/4/1976 during KASPEX-76 measured with the dropsonde (Foken and Kuznecov 1978). Stronger temperature fluctuations occurred in the height range 4–6 m. The reported turbulent sensible heat fluxes were measured at 6 m using the eddy-covariance method, and determined at the water surface from the temperature gradient in the molecular boundary layer



with variations in air temperature of 0.2–0.3 K is conspicuous. This experimental finding suggests that Kelvin–Helmholtz instabilities occur in this layer. The cause could be increased roughness due to capillary waves because of the relatively low wind speed (Roll 1948; Zilitinkevich et al. 2002). Further investigations are not possible due to the data situation, but the investigations of Chundshua and Andreev (1980) in the Black Sea can be confirmed.

3.2 The FINTUREX Results

3.2.1 Decoupling Near the Surface

Sodemann and Foken (2005) investigated the temperature structure near the snow surface and restricted themselves to a period from 27 January to 2 February 1994, during which sufficient quality-checked data were available. In particular, high wind speeds and snow drift (Foken 1998) prevented reliable turbulence measurements. Using the method described in Sect. 2.2.2, they found that occasional decoupling occurs near the snow surface. This means that the measured turbulent flux does not agree with the flux determined from the model approach using the temperature gradient between the measurement height and the surface (Fig. 5).

This decoupling occurred at low wind speeds and radiative cooling of the surface. Such a situation is shown in Fig. 6. In order to satisfy the decoupling criterion according to Eq. (1), missing standard deviations of the vertical velocity component had to be determined by parametrized values determined from the wind speed at a 10-m height with a regression analysis, based on known similarity relations for the standard deviation normalized by the friction velocity and the logarithmic wind profile as given in textbooks. The value w_{crit} changes by about one order of magnitude between the coupled and decoupled states, so that the decoupled region in Fig. 6 could be determined very well. From a wind speed below 3 ms^{-1} and very low solar altitudes, decoupling sets in below 2 m altitude, while above this approximately logarithmic temperature and wind profiles are maintained. From about 0200 to 0600 UTC, the 4 m height is also decoupled. Around 0800 UTC, decoupling is terminated by

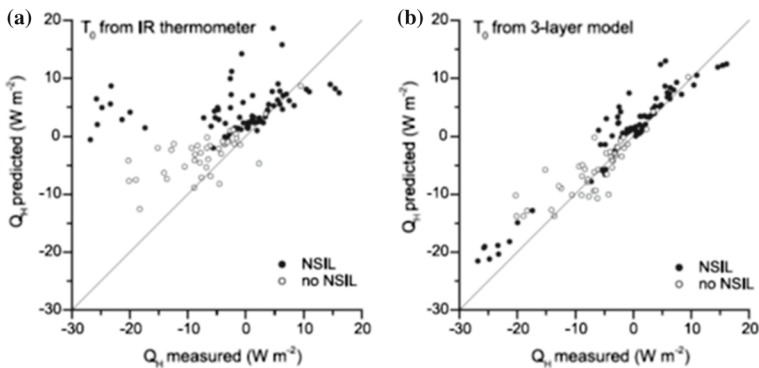


Fig. 5 Comparison of measured sensible heat flux Q_H at 2 m with predictions from a bulk model using the infrared (IR) surface temperature (a), and an estimate of the aerodynamic surface temperature from a three-layer temperature profile model (b). Data are classified into those where a near-surface inversion layer (NSIL) or decoupling was present (full dots) and absent (open dots). The line gives the 1:1 relation between measurements and observations. Figure from Sodemann and Foken (2005)

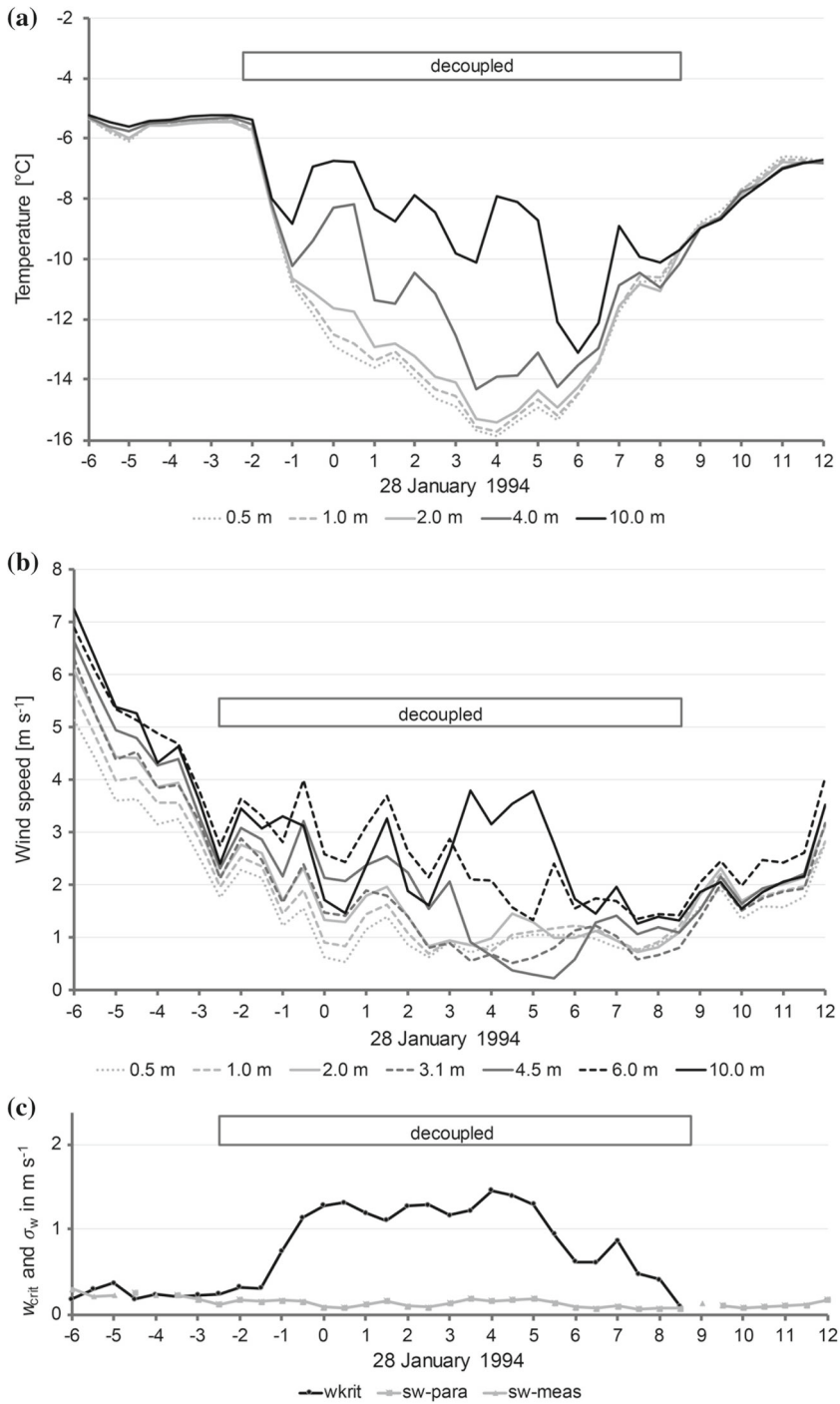


Fig. 6 Temperature (a) and wind (b) profiles from 27 January 1994 1800 UTC to 28 January 1994 1200 UTC with decoupled area indicated. The graph (c) shows the critical vertical velocity component for 2 m height according to Eq. (1) in black and the standard deviation of the vertical velocity component in grey with the measured values (triangles) and the parametrized values (squares)

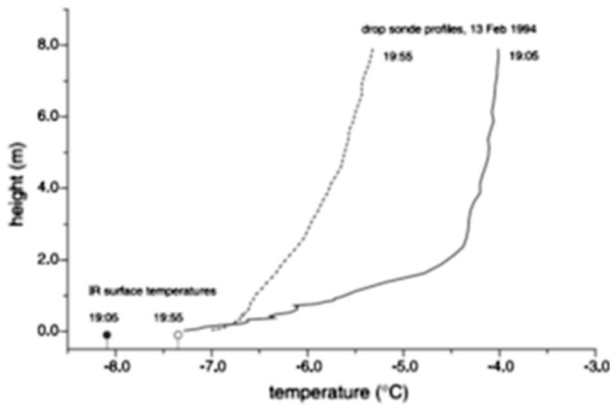


Fig. 7 Temperature structure over the snow surface during evening cooling on 13 February 1994, measured with a dropsonde (times in UTC). Circles mark the respective IR surface temperatures. The upper part of the temperature profile cooled due to the afternoon transition, with almost unchanged temperature gradients. The lower part apparently warmed up, because the longwave upward radiation at the surface increased due to high clouds. Figure from Sodemann and Foken (2005)

the higher sun elevations angle despite low wind speeds. In addition, Fig. 7 shows a striking example of low temperatures due to radiative cooling measured with the dropsonde, where high cloud cover alone can reduce strong cooling near the ground.

3.2.2 Temperature Inversion Near the Surface

Sodemann and Foken (2005) studied the vertical profile of the gradient Richardson number during the period indicated. In more stable cases, this proved to be largely constant in height. In nearly neutral cases, no uniform gradient Richardson number could be found. This was the case, among others, on 31 January 1994 until about 1900 UTC. For the period from 1200 to 1800 UTC, temperature profiles with an inversion at a height of about 2 m were shown. In the following, the measurements on 31 January are again subjected to a more extensive analysis.

Since the gradients were low with near-neutral stratification, a correction was made to the temperature (< 0.1 K) and wind (< 0.3 m s⁻¹) measurements by assuming a log-linear profile for the period of very high wind speeds from 0300 to 0700 UTC. As a result, the inversions found by Sodemann and Foken (2005) are weaker but still significant. To determine the gradient Richardson number, flux Richardson number and turbulent Prandtl number, gradients were assigned to the flux measurements at heights of 1.7 m, 4.2 m, and 11.6 m according to Table 2.

For a better assignment of the investigations to the meteorological conditions, see Fig. 8. The 31 January 1994 was a largely cloudless day with a maximum global radiation in the midday hours of almost 700 W m⁻² and an albedo of about 85%. During this period, even the net radiation was slightly positive. Wind speed was quite high at 8–10 m s⁻¹ from 0300 to 0800 UTC, then had values around 6–7 m s⁻¹ and decreased from 1200 UTC to values of about 4 m s⁻¹ at 1500 UTC. The temperature reached maximum values between 1200 and 1700 UTC of -1.5 °C, then decreased rapidly to values around -9 °C by midnight. The turbulent fluxes show gaps due to poor data quality in the early afternoon and evening. They showed largely similar values at all heights within the accuracy of the measurements. The

Table 2 Relation of wind speed and temperature gradients to flux measurements in the determination of Richardson number, Richardson flux number and turbulent Prandtl number

Height of flux measurements (m)	$\partial u / \partial z$	$\partial T / \partial z$
1.7	$[u(2\text{m}) - u(0.5\text{m})]/1.5\text{ m}$	$[T(2\text{m}) - T(0.5\text{m})]/1.5\text{ m}$
4.2	$[u(4.5\text{m}) - u(2\text{m})]/2.5\text{ m}$	$[T(4.5\text{m}) - T(2\text{m})]/2.5\text{ m}$
11.6	$[u(10\text{m}) - u(4.5\text{m})]/5.5\text{ m}$	$[T(10\text{m}) - T(4\text{m})]/6\text{ m}$

friction velocity largely follows the wind speed, but the decrease is more pronounced around 0800 UTC. From the wind speed and friction velocity measurements, a very small roughness length of 10^{-4} m is obtained. The sensible heat fluxes are very low, but the good agreement of the values at all three heights testifies that the measurements, although in the range usually assumed to be the detection limit (Foken et al. 2012), are reliable measurements after all. They were -10 W m^{-2} at night and reached positive values of up to about 5 W m^{-2} from 1200 to 1500 UTC.

The parameters and similarity numbers given in Sect. 2.2.3 are shown in Fig. 9. The Obukhov–Lettau stability parameter z/L (Foken and Börngen 2021) indicates slightly stable stratification until 1200 UTC, slightly unstable stratification analogous to the sensible heat flux from 1200 to 1500 UTC, and more stable stratification in the late afternoon. The gradient Richardson number also indicates stable stratification except for at 1200 to 1500 UTC. However, at 4.2 m, the values from 0900 to 1700 UTC are slightly unstable. The Richardson flux number follows the sensible heat flux, but without height constancy. The values at a height of 1.7 m are the largest in magnitude, while those at 11.6 m are the smallest. The turbulent Prandtl number exhibits values < 1 until 0900 UTC, as known from the literature (Foken 2017, overview in Table 2.6). Thereafter, the values increase significantly and reach values < 1 again in the late afternoon. To determine the eddy conductivity according to Eq. (9), the sensible heat flux and the temperature gradient must have the same sign. Due to the temperature inversion present, this is not always the case. For these situations, the turbulent Prandtl number was determined with the modulus of K_h and labelled the turbulent counter-gradient Prandtl number.

Analogous to Sodemann and Foken (2005), Fig. 10a shows the vertical temperature profiles from 10-min averages, but already from 0800 UTC. The corresponding wind profiles are shown in Fig. 10b. At still-high wind speeds around 0800 UTC, the temperature profile is largely log-linear, also from 1800 UTC. From 1000 to 1600 UTC, an inversion forms at a height of about 1–2 m. During this period, the wind profiles are largely log-linear, as they are during the high wind speeds from 0300 to 0600 UTC (not shown here). The wind profiles at 0800 and 1800 UTC, which deviate from this shape, are seen in connection with the change in wind speed, which always leads to a change in surface structure (zastруги) and thus to the formation of low internal boundary layers.

Finally, Fig. 11 shows the same relationships as Fig. 3, which is a copy of Zilitinkevich et al. (2013), but with data from FINTUREX on 31 January 1994. Only data for $Ri > 0$ are shown. However, the data are all within a range of gradient Richardson number less than the critical Richardson number ($Ri < Ri_c = 0.2$). The data for a height of 1.7 m a.g.l. satisfy the usual relation between Ri and Rf and thus also the model of Zilitinkevich et al. (2013). The data for 4.2 m and 11.6 m deviate from this because of the modified temperature gradients and generally small differences and fluxes. The dependence between the gradient Richardson number and the turbulent Prandtl number also includes measured data from Antarctica (Yagüe

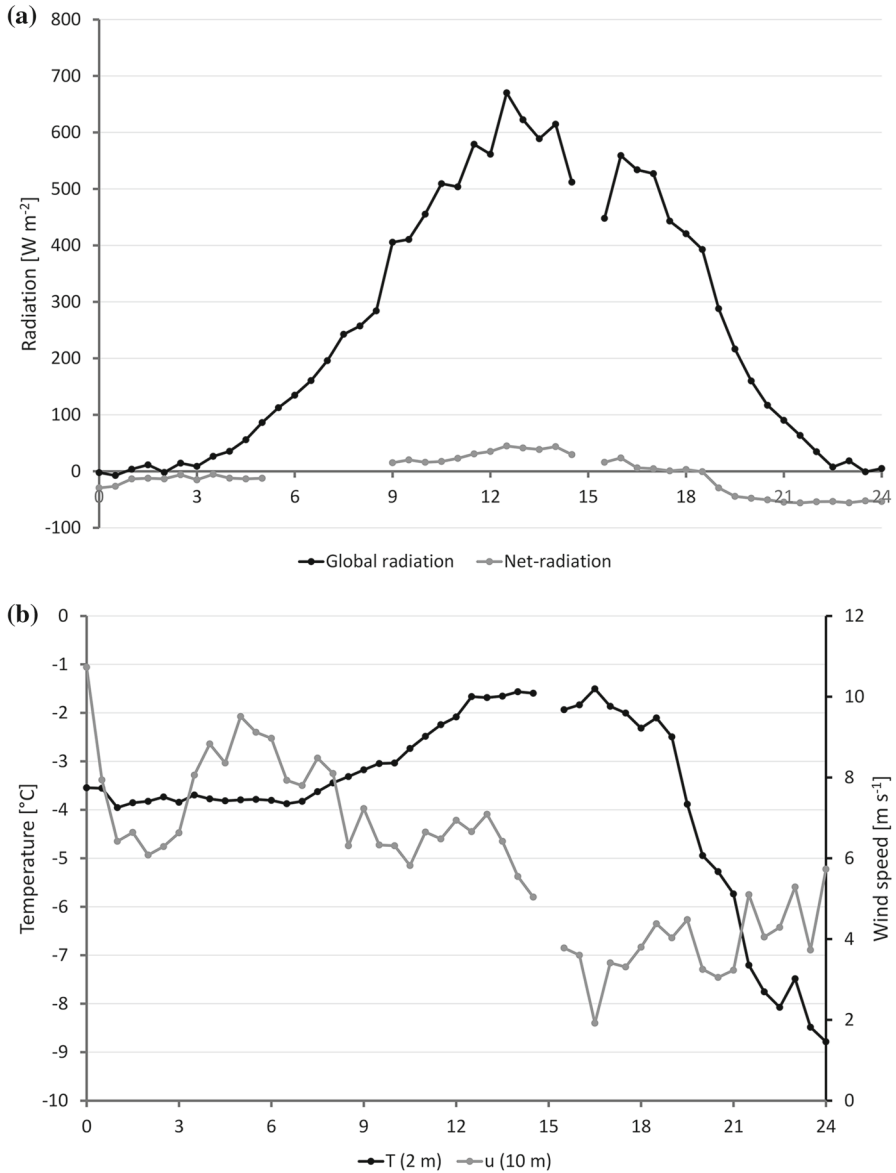


Fig. 8 Diurnal variation of important meteorological elements on 31 January 1994 during FINTUREX: global radiation and net radiation (a), air temperature at 2 m and wind speed at 10 m above ground level (a.g.l.) (b), friction velocity at 1.7 m, 4.2 m, and 11.6 m a.g.l. (c) and sensible heat flux in kinematic units at 1.7 m, 4.2 m und 11.6 m a.g.l. (d)

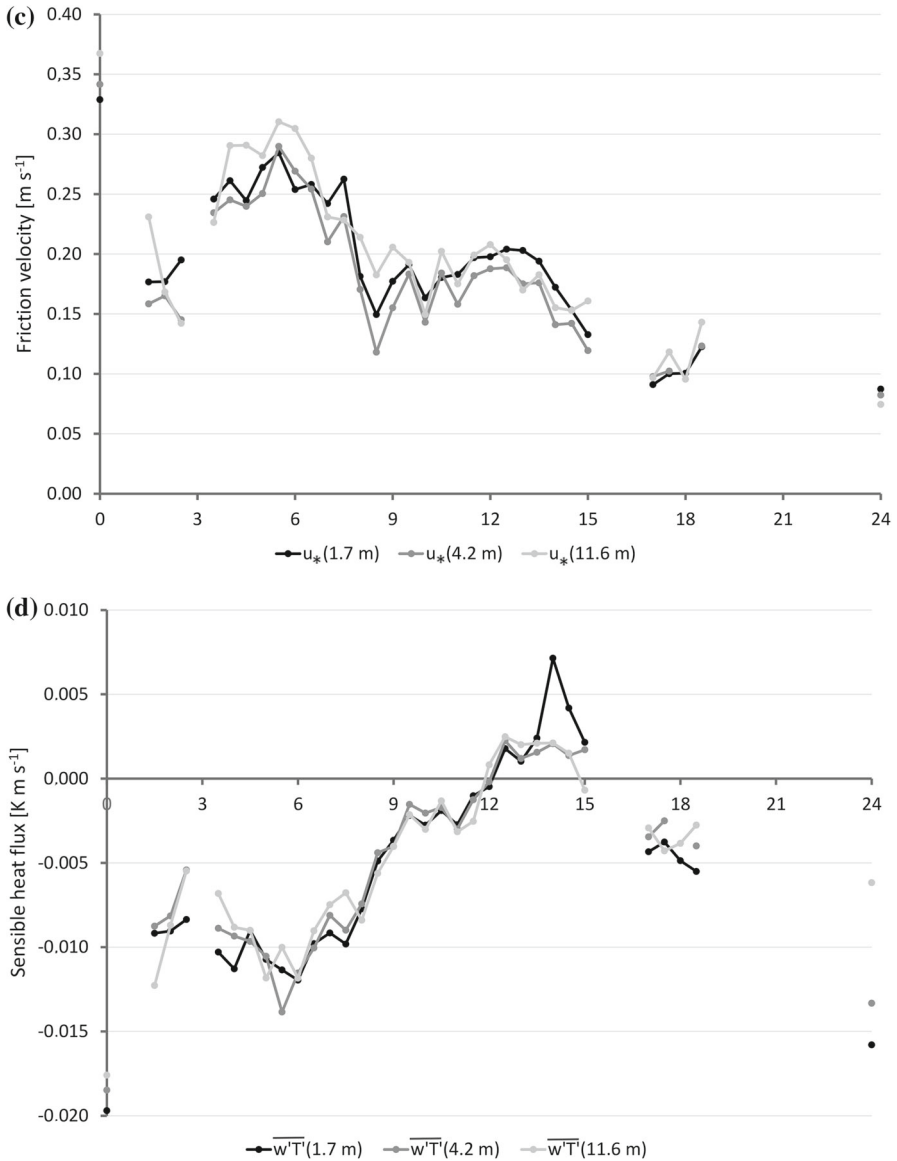


Fig. 8 continued

and Cano 1994) and from a katabatic flow (Monti et al. 2002), but only class averages. For FINTUREX, the 30-min values were plotted. It was deliberately not averaged to show that values $\text{Pr}_T > 1$ occur. As can be seen in Fig. 9d, these values occur under special conditions with inversion layer and do not represent a scattering of the measured values.

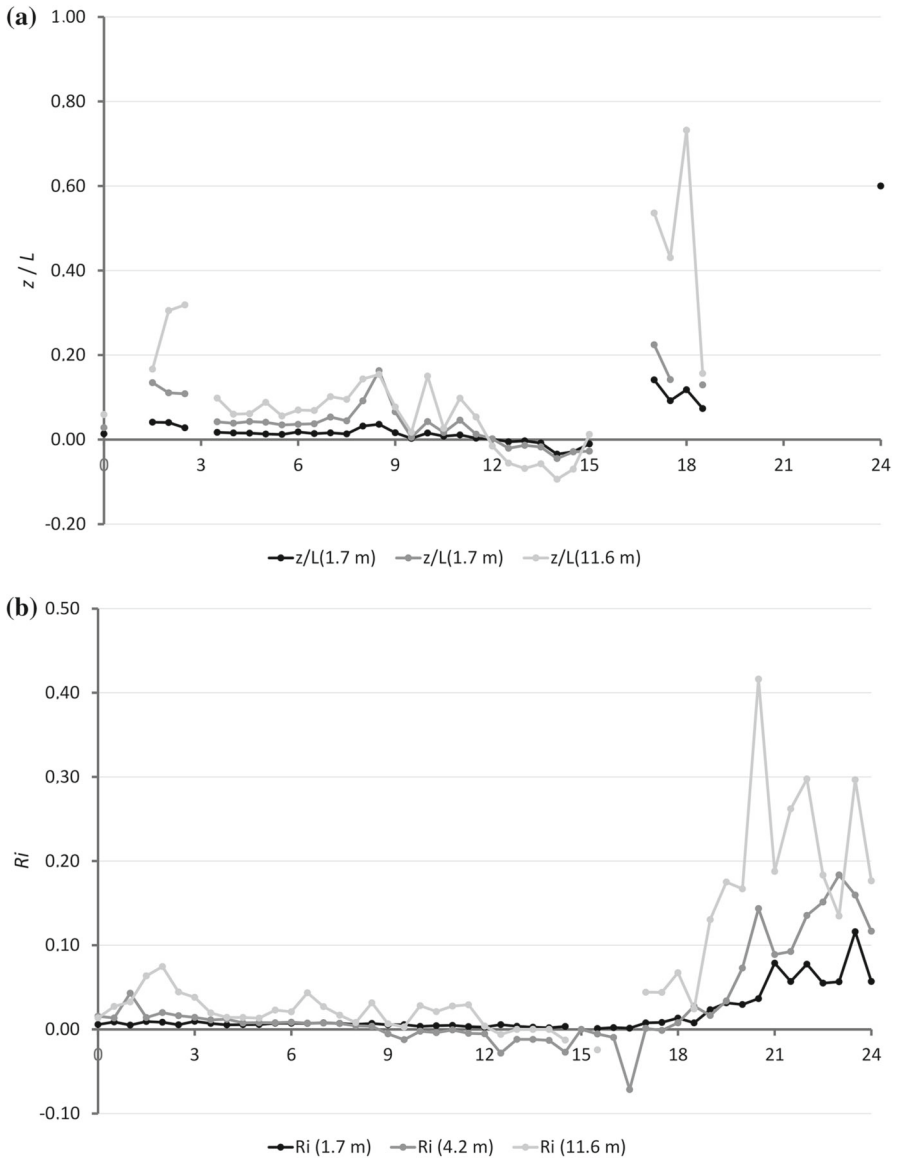


Fig. 9 Diurnal variation of calculated meteorological variables at 1.7 m, 4.2 m and 11.6 m a.g.l. on 31 January 1994 during FINTUREX: **(a)** local Obukhov-Lettau stability parameter, **(b)** gradient Richardson number, **(c)** Richardson flux number and **(d)** turbulent Prandtl number and turbulent counter-gradient (CG) Prandtl number (see text)

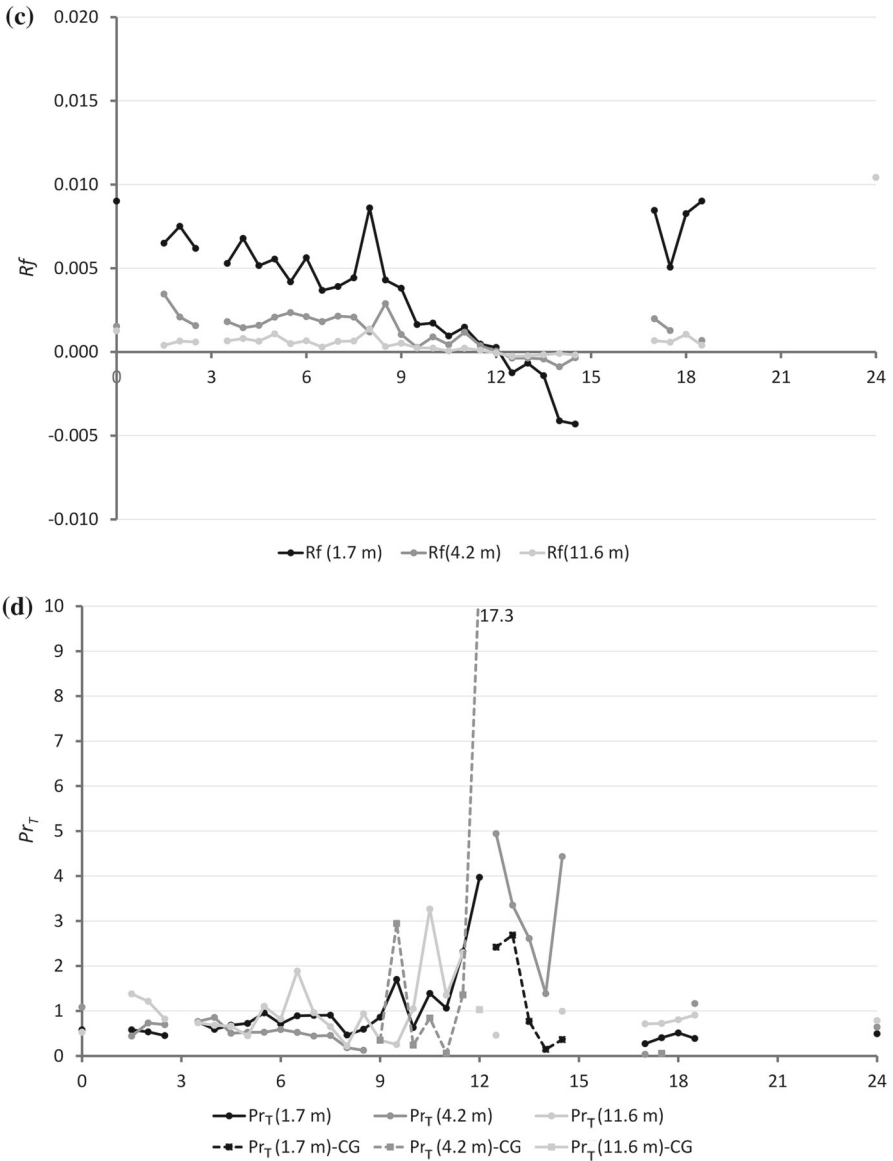


Fig. 9 continued

4 Discussion

4.1 Decoupling Near the Surface

The example of decoupling near the surface due to radiative cooling (Garratt and Brost 1981) is very typical and is described several times in the literature, including some examples in the classical microclimatic literature (Geiger et al. 2009; Geiger 2013). Such measurements

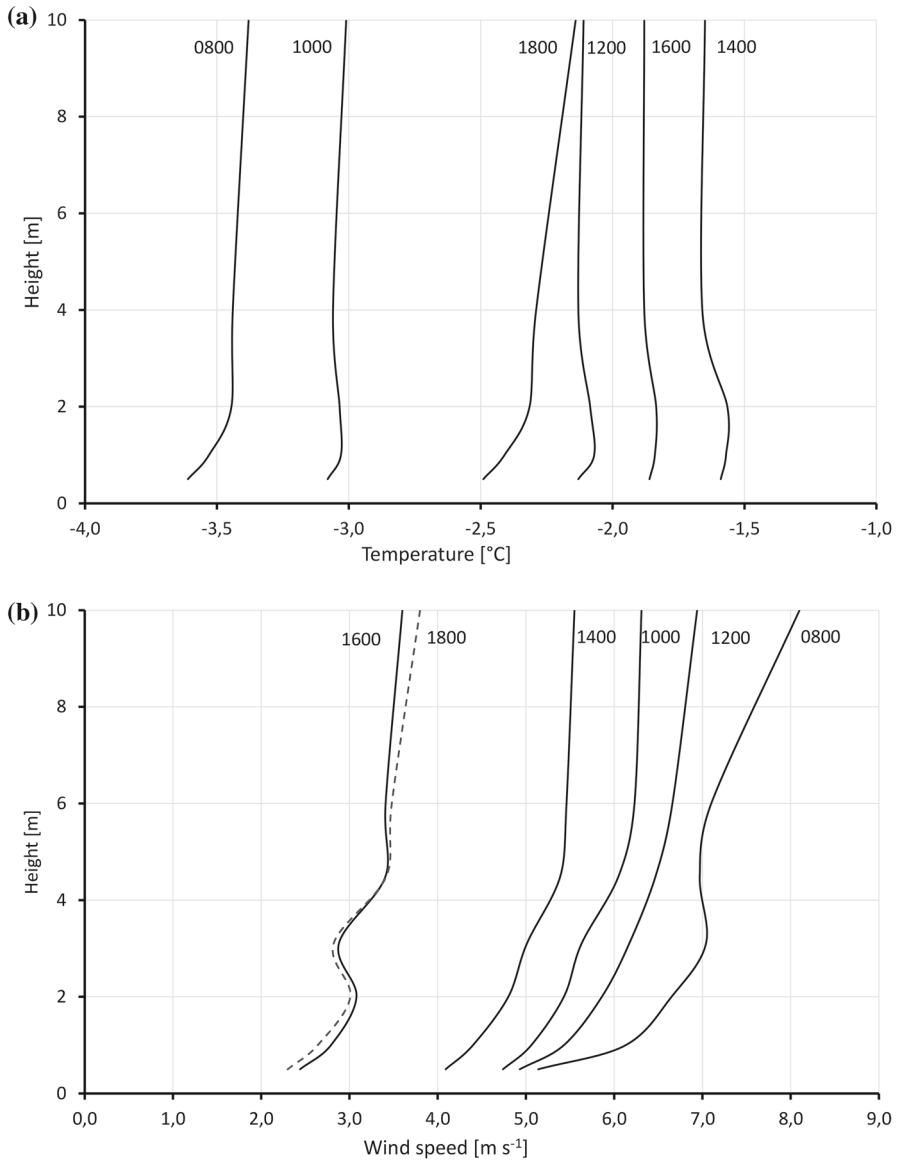


Fig. 10 Vertical profiles of air temperature (a) and wind speed (b) at selected times (a 10-min average) on 31 January 1994 during FINTUREX

are also available for Antarctica, e.g. in Kottmeier and Belitz (1987) from 1983 to 1987 from a 45-m-high tower at Neumayer I Station, an example for 28 August 1883 is shown by Handorf (1996). Such studies have apparently not been published for the SHEBA experiment. For the CASES-99 experiment (Poulos et al. 2002), to study the stable nocturnal boundary layer over grassland in Kansas in October 1999, Sun et al. (2003) conducted such studies. The CASES-99 experiment has been extensively studied, also recently with respect to wind

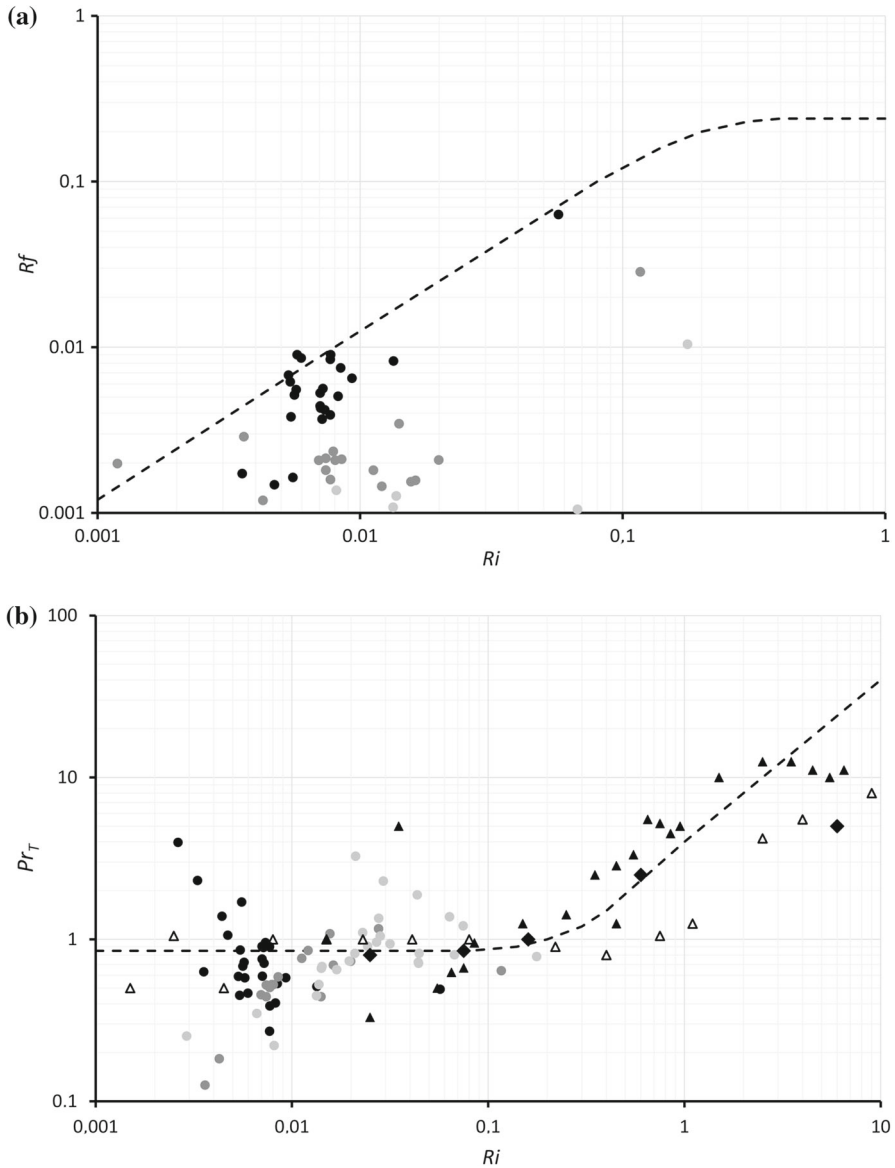


Fig. 11 By analogy with Fig. 3, plots of the dependence of the Richardson flux number on the gradient Richardson number (a) and the turbulent Prandtl number on the gradient Richardson number (b). Circles: 31 January 1994 during FINTUREX, black at 1.7 m, dark grey at 4.2 m and light grey at 11.6 m a.g.l.; triangles: binned values at a slope according to Monti et al. (2002); diamonds: binned values at the Halley Station, Antarctica, 1986, according to Yagüe and Cano (1994); unfilled triangles: binned values at SHEBA according to Grachev et al. (2007)

conditions under these conditions (Hicks 2022). Many such studies are available but cannot all be mentioned here. I have included the problem in this work, and, for these cases, it was clear that the decoupling test works well and gives significant results.

4.2 Temperature Inversion Near the Surface

There are currently several papers showing near-surface inversions and thus possible decoupling (Andreev et al. 1969; de La Casinière 1974; Foken and Kuznecov 1978; Chundshua and Andreev 1980; Halberstam and Schiedge 1981; Sodemann and Foken 2005; Lüers and Bareiss 2010), so it is not a single artefact. In search of a valid technical justification for this, the work of Basu and Holtslag (2021), and thus that of Zilitinkevich et al. (2013), seem to be on target. While, in general, $Pr_T < 1$ is assumed, the developed model contains regions with $Pr_T > 1$. This means that momentum transport predominates over the heat transport ($K_m > K_h$). Impressively, Monti et al. (2002) were able to show this, as sufficiently high wind speeds were still present for $Ri > Ri_c$ due to the katabatic flow, even with radiation-induced stabilization. Such katabatic runoff shows a pronounced wind maximum near the surface (Shapiro and Fedorovich 2007; Fedorovich and Shapiro 2009), which may also be associated with changes in the temperature gradient. This could not be shown by Monti et al. (2002) because of only two measurement heights. The Neumayer Station has no katabatic winds, so that with the beginning of stabilization the wind speed decreases, as could also be seen for 31 January after 1800 UTC.

The experimental investigations mentioned above consistently show a very low roughness parameter in the order of 10^{-3} to 10^{-4} m, and thus a strong decrease in wind speed immediately above the surface. This obviously justifies high values of K_m , while the sensible heat flux is very low and so is K_h , resulting in the formation of an inversion and high turbulent Prandtl numbers. However, energy conservation is only guaranteed if the thermal energy is balanced through a counter-gradient situation. This can be realized by coherent structures, by which larger amounts of energy are exchanged during very short time intervals and locally without changing the gradient. Coherent structures are not atypical over snow surfaces and could be found for FINTUREX at typical frequencies of 1 Hz using wavelet studies (Handorf and Foken 1997). However, coherent structures are also observed in the context of Kelvin–Helmholtz instabilities, as clearly occurred with KASPEX-76 (see Fig. 4). Unfortunately, a combination of both investigations on the same dataset is not possible, as 30 years ago mass data storage was not as easy as it is today. Such situations can be modelled with higher-order closure models; this has at least been demonstrated for counter gradients in forests (Falge et al. 2017). The existing dataset is not sufficient to explore this further.

Combining Fig. 8d and Fig. 10a, a typical picture for counter-gradient fluxes (Brunet 2020) is obtained in Fig. 12, similar to that shown in Fig. 4 for KASPEX-76 at 6 m above the sea surface. At 0800 UTC, gradients and sensible heat fluxes show the typical slightly stable case. At 1000 UTC, counter-gradient fluxes are found at the lower measurement height of 1.7 m and extending to the middle measurement height of 4.2 m at 1200 UTC. At 11.7 m, there is already slightly unstable stratification. The unstable stratification dominates thereafter, with counter-gradient fluxes in the opposite direction occurring at 1400 UTC at the lower measurement height. Due to the decreasing wind speed (Fig. 8b) in the afternoon, quality-assured turbulence measurement data are missing. At 1800 UTC, slightly stable conditions analogous to 0800 UTC are again present. The coupling test according to Eq. (1) resulted in a decoupling only after 1900 UTC, as can also be clearly seen from the gradient Richardson number (Fig. 9b).

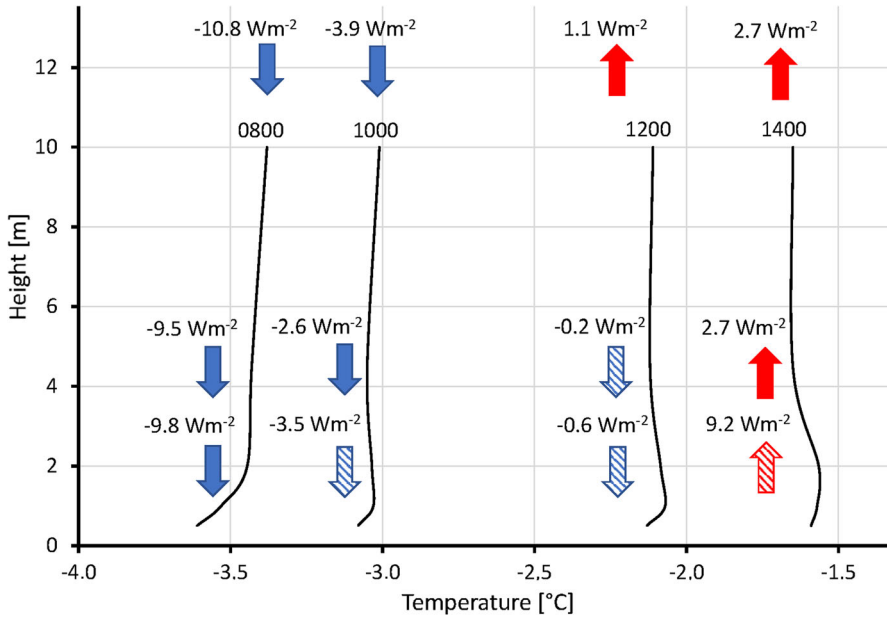


Fig. 12 Plot of selected vertical temperature profiles and sensible heat fluxes for FINTUREX on 31 January 1994, where tightened arrows for the sensible heat flux are counter-gradient fluxes, i.e. the temperature gradient has the opposite sign to that of the turbulent flux

5 Conclusion

This study has shown that (i) strong near-surface temperature gradients caused by radiative cooling and (ii) near-surface temperature inversions are two physically completely different processes. In the first case (i), as shown, we are dealing with decoupling, where the sensible heat fluxes are very small and non-steady state, so they often cannot be considered as certain because of data quality issues. Here, what is unfortunately no longer possible for FINTUREX, a high temporal resolution determination of the fluxes by wavelet analysis would be appropriate (Schaller et al. 2017). The second case (ii) is clearly about counter-gradient fluxes and high turbulent Prandtl numbers, which have only been investigated for high vegetation up to now, except in KASPEX-76 (Foken and Kuznetsov 1978) and the FINTUREX experiment in Antarctica. Because of the very low gradients and low fluxes, apparently little attention has been paid to this phenomenon. Such investigations are probably not possible with the measurements at the Halley Research Station, since the lowest measurement height was already 5 m (King 1990; King and Anderson 1994). However, it would certainly be useful to look again at the SHEBA dataset (Persson et al. 2002), since measurements were made there at least at 2.2 m, 3.2 m and 5.1 m. The differences in the determined universal functions as a function of Obukhov length and local Obukhov length (Grachev et al. 2005) for Richardson numbers greater than the critical Richardson number suggest such cases. It would also be interesting for CASES-99, because of the presence of katabatic winds in the slightly inclined terrain (Sun et al. 2003), to see if a similar investigation could be carried out like by Monti et al. (2002). In this sense, this paper should also be a stimulus for the further analysis of

existing datasets. With the work of Zilitinkevich et al. (2013) some theoretical justification is also given by the possibility of values of $Pr_T > 1$.

The practical significance of the investigations carried out emerges as two aspects. (i) The high temperature gradients with stable stratification are associated with only low sensible heat fluxes due to decoupling. A flux calculation using a bulk approach would lead to much higher sensible heat fluxes. This could be avoided by using the test for decoupling according to Peltola et al. (2021). This test is significant enough that simply parametrizations of the missing standard deviation of the vertical velocity component can be done. In the present case, a standard deviation of the vertical wind component as 5% of the wind speed at 10 m would have been a sufficiently accurate parametrizations (Fig. 6c). (ii) Cases with an inversion close to the ground would be treated as neutral cases by models, even for models very well fitted to the measured data (Gryanik et al. 2021), as the model layers are significantly higher than the relevant range of 1 m to 5 m height. However, the experimental data show that, when the net radiation is positive, these are certainly associated with positive sensible heat fluxes. With the generally low turbulent fluxes over snow and ice, there could be associated dew processes that go unrecognized in the modelling. Thus, in the context of increased thawing of glaciers and fast ice, attention should be paid to these cases. Consequently, the phenomena worked on can hardly be applied in climate and weather prediction models, but they can be significant in experimental process studies and adapted modelling.

A general shortcoming in measurement experiments was a lack of measurements at low heights (0.5–3 m), so that inversion layers near the ground could not be detected. In addition, there must be relatively high measurement accuracy to reliably identify the weak gradients. Limitations for gradient and flux measurements in this altitude range are disturbances due to snow drift (Foken 1998; Burns et al. 2012; Sigmund et al. 2022), so that the data cannot be evaluated continuously. In addition, the surface must be relatively smooth (shelf or fast ice), so that such measurements are not suitable over areas with pack ice. Optical-fiber-based distributed sensing (OFDS) was developed in recent years as a reliable measurement method (Thomas and Selker 2021), so it would be possible to design experiments specifically for this purpose. This could be shown for the strong near-ground gradients in stable stratification (Lapo et al. 2022), and near-ground inversions may yet be determined from such datasets.

Acknowledgements The KASPEX campaigns in 1975 and 1976 were funded by the Institute of Oceanology, Moscow, the University of Leipzig, and the Council for Mutual Economic Assistance (Comecon); the FINTUREX campaign in 1994 was funded by the German Meteorological Service, Offenbach, and the Alfred-Wegener Institute, Bremerhaven. The article is dedicated to the memory of Sergey S. Zilitinkevich, who was very interested in the results of FINTUREX. Appropriate coefficients were determined for his model (Zilitinkevich and Calanca 2000) using this dataset (Sodemann and Foken 2004).

Funding Open Access funding enabled and organized by Projekt DEAL. Open Access funding enabled and organized by Projekt DEAL.

Data Availability The datasets analysed during the current study are available from the author on reasonable request.

Declaration

Conflict of interest The author has declared that he has any competing interests.

Open Access This article is licensed under a Creative Commons Attribution 4.0 International License, which permits use, sharing, adaptation, distribution and reproduction in any medium or format, as long as you give appropriate credit to the original author(s) and the source, provide a link to the Creative Commons licence, and indicate if changes were made. The images or other third party material in this article are included in the

article's Creative Commons licence, unless indicated otherwise in a credit line to the material. If material is not included in the article's Creative Commons licence and your intended use is not permitted by statutory regulation or exceeds the permitted use, you will need to obtain permission directly from the copyright holder. To view a copy of this licence, visit <http://creativecommons.org/licenses/by/4.0/>.

References

- Acevedo OC, Mahrt L, Puhales FS, Costa FD, Medeiros LE, Degrazia GA (2016) Contrasting structures between the decoupled and coupled states of the stable boundary layer. *Q J R Meteorol Soc* 142:693–702. <https://doi.org/10.1002/qj.2693>
- Andreas EL (2002) Parametrizing scalar transfer over snow and ice: a review. *J Hydrometeorol* 3:417–432. [https://doi.org/10.1175/1525-7541\(2002\)003%3c0417:PSTOSA%3e2.0.CO;2](https://doi.org/10.1175/1525-7541(2002)003%3c0417:PSTOSA%3e2.0.CO;2)
- Andreev EG, Lavorko VS, Pivovarov AA, Chundshua GG (1969) O vertikalnom profile temperaturey vblizi granicy rasdela more - atmosfera (About the vertical temperature profile close to ocean–atmosphere interface). *Okeanologija* 9:348–352
- Basu S, Holtslag AAM (2021) Turbulent Prandtl number and characteristic length scales in stably stratified flows: steady-state analytical solutions. *Environ Fluid Mech* 21:1273–1302. <https://doi.org/10.1007/s10652-021-09820-7>
- Baum W, Foken T, Lattauschke J, Rettig W, Mattern W (1994) Entwicklung, Bau und Test eines Vertikalpsychrometers. *Dt Wetterdienst, Forsch. Entwicklung, Arbeitsergebnisse*. 12:18
- Bjunter EK (1974) Teoreticeskij rascet soprotivlenija morskoy poverchnosti (Theoretical calculation of the resistance at the surface of the ocean). In: Dubov AS (ed) *Processy perenosa vblizi poverchnosti razdela okean - atmosfera* (Exchange processes near the ocean–atmosphere interface). *Gidrometeoizdat, Leningrad*, pp 66–114
- Bovsheverov VM, Voronov VP (1960) Akusticheskii fljuzer (Acoustic rotor). *Izv AN SSSR, Ser Geofiz* 6:882–885
- Brömme G, Woitzik B, Jörn M, Schindler V (1991) Feinanemometer für mikrometeorologische Anwendungen. *Abh Meteorol Dienstes DDR* 146:23–26
- Bruch H (1940) Die vertikale Verteilung der Windgeschwindigkeit und der Temperatur in den untersten Metern über der Wasseroberfläche. In: *Veröffentlichungen des Instituts für Meereskunde der Univ. Berlin, Reihe A.*, vol 38, p 66
- Brunet Y (2020) Turbulent Flow in plant canopies: historical perspective and overview. *Boundary-Layer Meteorol* 177:315–364. <https://doi.org/10.1007/s10546-020-00560-7>
- Burns SP, Horst TW, Jacobsen L, Blanken PD, Monson RK (2012) Using sonic anemometer temperature to measure sensible heat flux in strong winds. *Atmos Meas Tech* 5:2095–2111. <https://doi.org/10.5194/amt-5-2095-2012>
- Chundshua GG, Andreev EG (1980) O mehanizme formirovaniya inversii temperaturey v privodnoim sloe atmosfery nad morem (About a mechanism of the development of a temperature inversion in the near surface layer above the ocean). *Dokl AN SSSR* 255:829–832
- Däke CU (1972) Über ein neues Modell des Strahlungsbilanzmessers nach Schulze. *Ber Dt Wetterdienstes* 126:2–22
- de La Casinière AC (1974) Heat exchange over a melting snow surface. *J Glaciol* 13:55–72. <https://doi.org/10.3189/S0022143000023376>
- Denmead DT, Bradley EF (1985) Flux-gradient relationships in a forest canopy. In: Hutchison BA, Hicks BB (eds) *The forest–atmosphere interaction*. D. Reidel Publishing Company, Dordrecht, pp 421–442
- Falge E, Köck K, Gatzsche K, Voß L, Schäfer A, Berger M, Dlugi R, Raabe A, Pyles RD, Paw UKT, Foken T (2017) Modelling of energy and matter exchange. In: Foken T (ed) *Energy and matter fluxes of a spruce forest ecosystem, ecological studies*, vol 229. Springer, Cham, pp 379–414. https://doi.org/10.1007/978-3-319-49389-3_16
- Fedorovich E, Shapiro A (2009) Structure of numerically simulated katabatic and anabatic flows along steep slopes. *Acta Geophys* 57:981–1010. <https://doi.org/10.2478/s11600-009-0027-4>
- Finnigan J (2000) Turbulence in plant canopies. *Ann Rev Fluid Mech* 32:519–571. <https://doi.org/10.1146/annurev.fluid.32.1.519>
- Foken T (1975) Die Messung der Mikrostruktur der vertikalen Lufttemperaturverteilung in unmittelbarer Nähe der Grenze zwischen Wasser und Atmosphäre. *Z Meteorol* 25:292–295
- Foken T (1978) The molecular temperature boundary layer of the atmosphere over various surfaces. *Archiv Meteorol Geophys Bioklim Ser A* 27:59–67. <https://doi.org/10.1007/BF02246461>

- Foken T (1979) Vorschlag eines verbesserten Energieaustauschmodells mit Berücksichtigung der molekularen Grenzschicht der Atmosphäre. *Z Meteorol* 29:32–39
- Foken T (1984) The parametrisation of the energy exchange across the air-sea interface. *Dyn Atmos Oceans* 8:297–305. [https://doi.org/10.1016/0377-0265\(84\)90014-9](https://doi.org/10.1016/0377-0265(84)90014-9)
- Foken T (1998) Bestimmung der Schneedrift mittels Ultraschallanemometern. *Ann Meteorol* 37(2):451–452
- Foken T (2002) Some aspects of the viscous sublayer. *Meteorol Z* 11:267–272. <https://doi.org/10.1127/0941-2948/2002/0011-0267>
- Foken T (2003) Besonderheiten der Temperaturstruktur nahe der Unterlage. In: Chmielewski F-M, Foken T (eds) Beiträge zur Klima- und Meeresforschung. Eigenverlag Chmielewski & Foken, Berlin und Bayreuth, pp 103–112. https://doi.org/10.15495/EPub_UBT_00006610
- Foken T (2006) 50 Years of the Monin–Obukhov similarity theory. *Boundary-Layer Meteorol* 119:431–447. <https://doi.org/10.1007/s10546-006-9048-6>
- Foken T (2017) *Micrometeorology*. Springer, Berlin, p 362. <https://doi.org/10.1007/978-3-642-25440-6>
- Foken T, Börngen M (2021) Lettau's contribution to the Obukhov Length Scale: a scientific historical study. *Boundary-Layer Meteorol* 179:369–383. <https://doi.org/10.1007/s10546-021-00606-4>
- Foken T, Kuznecov OA (1978) Die wichtigsten Ergebnisse der gemeinsamen Expedition "KASPEX-76" des Institutes für Ozeanologie Moskau und der Karl-Marx-Universität Leipzig. *Beitr Meeresforsch* 41:41–47
- Foken T, Wichura B (1996) Tools for quality assessment of surface-based flux measurements. *Agric for Meteorol* 78:83–105. [https://doi.org/10.1016/0168-1923\(95\)02248-1](https://doi.org/10.1016/0168-1923(95)02248-1)
- Foken T, Kitajgorodskij SA, Kuznecov OA (1978) On the dynamics of the molecular temperature boundary layer above the sea. *Boundary-Layer Meteorol* 15:289–300. <https://doi.org/10.1007/BF02652602>
- Foken T, Leuning R, Oncley SP, Mauder M, Aubinet M (2012) Corrections and data quality. In: Aubinet M et al (eds) *Eddy covariance: a practical guide to measurement and data analysis*. Springer, Dordrecht, pp 85–131. https://doi.org/10.1007/978-94-007-2351-1_4
- Garratt JR, Brost RA (1981) Radiative Cooling Effects within and above the Nocturnal Boundary Layer. *J Atmos Sci* 38:2730–2746. [https://doi.org/10.1175/1520-0469\(1981\)038%3c2730:RCEWAA%3e2.0.CO;2](https://doi.org/10.1175/1520-0469(1981)038%3c2730:RCEWAA%3e2.0.CO;2)
- Geiger R (2013) *Das Klima der bodennahen Luftschicht*. Springer Vieweg, Wiesbaden, p 646. <https://doi.org/10.1007/978-3-658-03519-8>
- Geiger R, Aron RH, Todhunter P (2009) *The climate near the ground*. Rowman & Littlefield, Lanham, XVIII, p 623
- Grachev AA, Fairall CW, Persson POG, Andreas EL, Guest PS (2005) Stable boundary-layer scaling regimes: the Sheba data. *Boundary-Layer Meteorol* 116:201–235. <https://doi.org/10.1007/s10546-004-2729-0>
- Grachev AA, Andreas EL, Fairall CW, Guest PS, Persson POG (2007) On the turbulent Prandtl number in the stable atmospheric boundary layer. *Boundary-Layer Meteorol* 125:329–341. <https://doi.org/10.1007/s10546-007-9192-7>
- Grachev AA, Andreas EL, Fairall CW, Guest PS, Persson POG (2012) Outlier problem in evaluating similarity functions in the stable atmospheric boundary layer. *Boundary-Layer Meteorol* 144:137–155. <https://doi.org/10.1007/s10546-012-9714-9>
- Gross G (2021) On the importance of a viscous surface layer to describe the lower boundary condition for temperature. *Meteorol Z* 30:271–278. <https://doi.org/10.1127/metz/2021/1073>
- Gryanik VM, Lüpkens C, Sidorenko D, Grachev A (2021) A universal approach for the non-iterative parametrization of near-surface turbulent fluxes in climate and weather prediction models. *J Adv Model Earth Syst* 13:e2021MS002590. <https://doi.org/10.1029/2021MS002590>
- Gurjanov AE, Zubkovskij SL, Fedorov MM (1984) Mnogokanalnaja avtomatizirovannaja sistema obrabotki signalov na baze EVM (Automatic multi-channel system for signal analysis with electronic data processing). *Geod Geophys Veröff, R II* 26:17–20
- Halberstam I, Schieldge JP (1981) Anomalous behavior of the atmospheric surface layer over a melting snow-pack. *J Appl Meteorol Climatol* 20:255–265. [https://doi.org/10.1175/1520-0450\(1981\)020%3c0255:ABOTAS%3e2.0.CO;2](https://doi.org/10.1175/1520-0450(1981)020%3c0255:ABOTAS%3e2.0.CO;2)
- Hanafusa T, Fujitana T, Kobori Y, Mitsuta Y (1982) A new type sonic anemometer-thermometer for field operation. *Papers Meteorol Geophys* 33:1–19
- Handorf D (1996) Zur Parametrisierung der stabilen atmosphärischen Grenzschicht über einem antarktischen Schelfeis. *Ber Polarforschung*. 204:133
- Handorf D, Foken T, Kottmeier C (1999) The stable atmospheric boundary layer over an Antarctic ice sheet. *Boundary-Layer Meteorol* 91:165–186. <https://doi.org/10.1023/A:1001889423449>
- Handorf D, Foken T (1997) Analysis of turbulent structure over an Antarctic ice shelf by means of wavelet transformation. In: 12th symposium on boundary layer and turbulence, Vancouver BC, Canada, 28 July–1 August 1997. American Meteorological Society, pp 245–246

- Hicks BB (2022) On kinematic isolation in stable stratification: the CASES-99 tower observations. *Boundary-Layer Meteorol* 183:67–77. <https://doi.org/10.1007/s10546-021-00677-3>
- Jocher G, Ottosson Löfvenius M, De Simon G, Hörnlund T, Linder S, Lundmark T, Marshall J, Nilsson MB, Näsholm T, Tarvainen L, Öquist M, Peichl M (2017) Apparent winter CO₂ uptake by a boreal forest due to decoupling. *Agric for Meteorol* 232:23–34. <https://doi.org/10.1016/j.agrformet.2016.08.002>
- King JC (1990) Some measurements of turbulence over an Antarctic ice shelf. *Q J R Meteorol Soc* 116:379–400. <https://doi.org/10.1002/qj.49711649208>
- King JC, Anderson PS (1994) Heat and water vapor fluxes and scalar roughness lengths over an Antarctic ice shelf. *Boundary-Layer Meteorol* 69:101–121. <https://doi.org/10.1007/BF00713297>
- King JC, Anderson PS, Smith MC, Mobbs SD (1996) The surface energy and mass balance at Halley, Antarctica during Winter. *J Geophys Res* 101(D14):19119–19128. <https://doi.org/10.1029/96JD01714>
- Koprov BM (2018) From the history of boundary-layer studies at the Institute of Atmospheric Physics. *Izv Atmos Oceanic Phys* 54:282–292. <https://doi.org/10.1134/S000143381803009X>
- Kottmeier C, Belitz H-J (1987) Meteorological research using a high mast on the Antarctic ice shelf. *Mar Technol* 1:5–10
- Lapo K, Freundorfer A, Fritz A, Schneider J, Olesch J, Babel W, Thomas CK (2022) The Large eddy Observatory, Voitsumra Experiment 2019 (LOVE19) with high-resolution, spatially distributed observations of air temperature, wind speed, and wind direction from fiber-optic distributed sensing, towers, and ground-based remote sensing. *Earth Syst Sci Data* 14:885–906. <https://doi.org/10.5194/essd-14-885-2022>
- Lüers J, Bareiss J (2010) The effect of misleading surface temperature estimations on the sensible heat fluxes at a high Arctic site—the Arctic Turbulence Experiment 2006 on Svalbard (ARCTEX-2006). *Atmos Chem Phys* 10:157–168. <https://doi.org/10.5194/acp-10-157-2010>
- Mahrt L, Thomas C, Richardson S, Seaman N, Stauffer D, Zeeman M (2013) Non-stationary generation of weak turbulence for very stable and weak-wind conditions. *Boundary-Layer Meteorol* 147:179–199. <https://doi.org/10.1007/s10546-012-9782-x>
- Monti P, Fernando HJS, Princevac M, Chan WC, Kowalewski TA, Pardyjak ER (2002) Observations of flow and turbulence in the nocturnal boundary layer over a slope. *J Atmos Sci* 59:2513–2534. [https://doi.org/10.1175/1520-0469\(2002\)059%3c2513:OOFATI%3e2.0.CO;2](https://doi.org/10.1175/1520-0469(2002)059%3c2513:OOFATI%3e2.0.CO;2)
- Peltola O, Lapo K, Thomas CK (2021) A physics-based universal indicator for vertical decoupling and mixing across canopies architectures and dynamic stabilities. *Geophys Res Lett* 48:e2020GL091615. <https://doi.org/10.1029/2020GL091615>
- Persson POG, Fairall CW, Andreas EL, Guest P, Perovich DK (2002) Measurements near the Atmospheric Surface Flux Group tower at SHEBA: near surface conditions and surface energy budget. *J Geophys Res.* <https://doi.org/10.1029/2000JC000705>
- Poulos GS, Blumen W, Fritts DC, Lundquist JK, Sun J, Burns SP, Nappo C, Banta R, Newsom R, Cuxart J, Terradellas E, Balsley B, Jensen M (2002) CASES-99: a comprehensive investigation of the stable nocturnal boundary layer. *Bull Am Meteorol Soc* 83:55–581. [https://doi.org/10.1175/1520-0477\(2002\)083%3c0555:CACIOT%3e2.3.CO;2](https://doi.org/10.1175/1520-0477(2002)083%3c0555:CACIOT%3e2.3.CO;2)
- Raupach MR, Finnigan JJ, Brunet Y (1996) Coherent eddies and turbulence in vegetation canopies: the mixing-layer analogy. *Boundary-Layer Meteorol* 78:351–382. https://doi.org/10.1007/978-94-017-0944-6_15
- Roll HU (1948) Wassernahes Windprofil und Wellen auf dem Wattenmeer. *Ann Meteorol* 1:139–151
- Schaller C, Göckede M, Foken T (2017) Flux calculation of short turbulent events—comparison of three methods. *Atmos Meas Tech* 10:869–880. <https://doi.org/10.5194/amt-10-869-2017>
- Shapiro A, Fedorovich E (2007) Katabatic flow along a differentially cooled sloping surface. *J Fluid Mech* 571:149–175. <https://doi.org/10.1017/S0022112006003302>
- Sigmund A, Dujardin J, Comola F, Sharma V, Huwald H, Melo DB, Hirasawa N, Nishimura K, Lehning M (2022) Evidence of strong flux underestimation by bulk parametrizations during drifting and blowing snow. *Boundary-Layer Meteorol* 182:119–146. <https://doi.org/10.1007/s10546-021-00653-x>
- Sodemann H, Foken T (2004) Empirical evaluation of an extended similarity theory for the stably stratified atmospheric surface layer. *Q J R Meteorol Soc* 130:2665–2671. <https://doi.org/10.1256/qj.03.88>
- Sodemann H, Foken T (2005) Special characteristics of the temperature structure near the surface. *Theor Appl Clim* 80:81–89. <https://doi.org/10.1007/s00704-004-0092-1>
- Sörgel M, Riederer M, Held A, Plake D, Zhu Z, Foken T, Meixner FX (2017) Trace gas exchange at the forest floor. In: Foken T (ed) *Energy and matter fluxes of a spruce forest ecosystem, ecological studies*, vol 229. Springer, Cham, pp 157–179. https://doi.org/10.1007/978-3-319-49389-3_8
- Sun J, Burns SP, Delany AC, Oncley SP, Horst TW, Lenschow DH (2003) Heat balance in the nocturnal boundary layer during CASES-99. *J Appl Meteorol* 42:1649–1666. [https://doi.org/10.1175/1520-0450\(2003\)042%3c1649:Hbitnb%3e2.0.CO;2](https://doi.org/10.1175/1520-0450(2003)042%3c1649:Hbitnb%3e2.0.CO;2)
- Sverdrup HU (1936) Das maritime Verdunstungsproblem. *Annalen Der Hydrographie Und Maritimen Meteorologie* 64:41–47

- Sverdrup HU (1937/38) On the evaporation from the ocean. *J Marine Res* 1:3–14
- Thomas C, Foken T (2007) Flux contribution of coherent structures and its implications for the exchange of energy and matter in a tall spruce canopy. *Boundary-Layer Meteorol* 123:317–337. <https://doi.org/10.1007/s10546-006-9144-7>
- Thomas CK, Selker J (2021) Optical-fiber-based distributed sensing methods. In: Foken T (ed) *Springer handbook of atmospheric measurements*. Springer Nature, Switzerland, pp 609–631. https://doi.org/10.1007/978-3-030-52171-4_20
- Yagüe C, Cano JL (1994) The influence of stratification on heat and momentum turbulent transfer in Antarctica. *Boundary-Layer Meteorol* 69:123–136. <https://doi.org/10.1007/BF00713298>
- Yagüe C, Maqueda G, Rees JM (2001) Characteristics of turbulence in the lower atmosphere at Halley IV station, Antarctica. *Dyn Atmos Oceans* 34:205–223. [https://doi.org/10.1016/S0377-0265\(01\)00068-9](https://doi.org/10.1016/S0377-0265(01)00068-9)
- Zilitinkevich SS, Calanca P (2000) An extended similarity theory for the stably stratified atmospheric surface layer. *Q J R Meteorol Soc* 126:1913–1923. <https://doi.org/10.1002/qj.49712656617>
- Zilitinkevich SS, Perov VL, King JC (2002) Near-surface turbulent fluxes in stable stratification: calculation techniques for use in general circulation models. *Q J R Meteorol Soc* 128:1571–1587. <https://doi.org/10.1002/qj.200212858309>
- Zilitinkevich SS, Elperin T, Kleerorin N, Rogachevskii I, Esau I (2013) A hierarchy of energy- and flux-budget (EFB) turbulence closure models for stably-stratified geophysical flows. *Boundary-Layer Meteorol* 146:341–373. <https://doi.org/10.1007/s10546-012-9768-8>

Publisher's Note Springer Nature remains neutral with regard to jurisdictional claims in published maps and institutional affiliations.